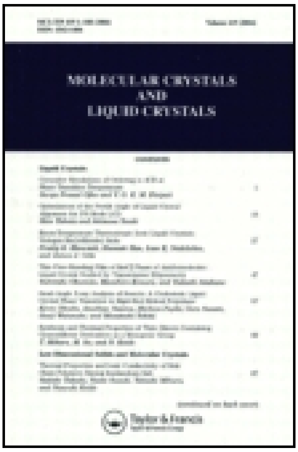

Molecular Crystals and Liquid Crystals Science and Technology. Section A. Molecular Crystals and Liquid Crystals
Publication details, including instructions for authors and subscription information:
http://www.tandfonline.com/loi/gmcl19

Surface-Anchortng Solitary Waves in Antiferroelectric Liquid Crystals

Yi-Kuo Yu [a], X. Y. Wang [a] & P. L. Taylor [a]
[a] Physics Department, Case Western Reserve University, Cleveland, Ohio, 44106-7079

Version of record first published: 04 Oct 2006

Mol. Cryst. Liq. Cryst., 1997, Vol. 301, pp. 177–182
Reprints available directly from the publisher
Photocopying permitted by license only

SURFACE-ANCHORING SOLITARY WAVES IN ANTIFERROELECTRIC LIQUID CRYSTALS

YI-KUO YU, X. Y. WANG AND P. L. TAYLOR
Physics Department, Case Western Reserve University
Cleveland, Ohio 44106-7079

Abstract By considering an expression for the energy of a cell containing an antiferroelectric smectic liquid crystal with only nearest-neighbor interactions between layers we conclude that while the transition to and from ferroelectric alignment can propagate as a stable solitary wave in the bulk of the material, under certain conditions a separate surface wave can also exist.

Following the experimental observation of propagating fingers of ferroelectric polarization in antiferroelectric liquid crystals (AFLCs) by Li *et al.*[1], we have recently proposed a theoretical account of this phenomenon[2]. We showed that the transition to and from ferroelectric alignment propagates as a stable solitary wave under certain conditions. In the present work we have extended our calculations to include the case of strong surface anchoring, and conclude that there may be two types of solitary wave. In addition to the bulk wave, in which the polarization of alternate smectic layers is reversed throughout the thickness of the cell containing the AFLC, we find that there can also be a surface wave in which the change in polarization is confined to a region close to the surface of the cell. The surface-anchored solitary waves move at a slower speed than their counterparts in the bulk.

In our model, the N smectic layers lie in the x-z plane as indicated in Fig. 1. The director is characterized by the constant angle θ_0 that it everywhere makes with the y axis and by the variable azimuthal angle $\phi_l(x,z)$ that it makes relative to the x axis in the x-z plane and in layer l. The Hamiltonian is then taken to be

$$\begin{aligned}\mathcal{H} &= D\sum_{l=1}^{N}\int dxdz\left\{\frac{k}{2}\left[\left(\frac{\partial\phi_l}{\partial x}\right)^2+\left(\frac{\partial\phi_l}{\partial z}\right)^2\right]+U\cos(\phi_l-\phi_{l-1})\right.\\ &+ b\sin(\phi_l-\phi_{l-1})-P_0E\cos\phi_l-\frac{\epsilon_0\Delta\epsilon\sin^2\theta_0}{2}E^2\sin^2\phi_l\\ &+ \left.W(z)\sin^2\phi_l+\frac{I}{2}\left(\frac{\partial\phi_l}{\partial t}\right)^2\right\}. \qquad (1)\end{aligned}$$

Here D is the layer thickness, k is an elastic constant, I is the moment of inertia per unit volume for rotation about the y axis, and $W(z)$ is a surface anchoring energy which we shall take to act only at the top and bottom surface of the cell, and thus to be of the form $w_0[\delta(z - d/2) + \delta(z + d/2)]$ with d the height of the cell. We assume planar anchoring, so that $w_0 > 0$. The elastic energy terms come from the variation of ϕ in the x-z plane. Because each layer is only one molecule thick, there is no variation of ϕ in the y direction within a layer. Instead there is the interlayer interaction, which is assumed to favor the herringbone structure[3,4] having an anti-parallel orientation of adjacent dipoles, as described by the term with coefficient U. Steric hindrance acts to introduce a small chiral deviation from a perfectly antiparallel orientation, and is represented by the term with the small coefficient b. Finally, the two terms containing the electric field E, which is assumed to be in the z direction, represent the effects of polarization and of the dielectric anisotropy, $\Delta\epsilon$, respectively, while ε_0 is the vacuum permittivity.

We add to the equations of motion obtained from the Hamiltonian (1) a dissipative term to account for the viscosity γ. The result is

$$\begin{aligned} I\frac{\partial^2\phi_l}{\partial t^2} + \gamma\frac{\partial\phi_l}{\partial t} &= k\left(\frac{\partial^2\phi_l}{\partial x^2} + \frac{\partial^2\phi_l}{\partial z^2}\right) - P_0 E \sin\phi_l \\ &+ \left(\frac{\varepsilon_0\Delta\epsilon\sin^2\theta_0}{2}E^2 - W(z)\right)\sin 2\phi_l \\ &+ U\left[\sin(\phi_l - \phi_{l-1} - \alpha) - \sin(\phi_{l+1} - \phi_l - \alpha)\right]. \end{aligned} \tag{2}$$

Here the antiferroelectric and chiral steric terms have been combined into a single set of terms by defining $\alpha \equiv \arctan(b/U)$ and approximating $\sqrt{U^2 + b^2}$ by U. The natural pitch of the helix formed by a sample with no boundaries and in zero field would then be $2\pi D/\alpha \simeq 2\pi DU/b$.

When α is small and the cell is not too thick, the ground state of the AFLC has $\phi_l = 0$ for all odd l and $\phi_l = \pi$ for all even l in the absence of an electric field. Application of an electric field lowers the energy of the ferroelectrically aligned state in which all $\phi_l = 0$. The critical electric field at which the ferroelectrically aligned state is reduced in energy below the antiferroelectric state is $E_{c2} = 2U/P_0$. When a region of ferroelectrically aligned material is formed, it will tend to spread by a process of domain-wall propagation along the layer in the x direction. In order to examine this process we consider a system where ϕ_l is constrained to be zero for l odd, and examine the dependence of the ϕ_l for even l on x, z, and t. Equation (2) then takes the form

$$I\frac{\partial^2\phi_l}{\partial t^2} + \gamma\frac{\partial\phi_l}{\partial t} - k\left(\frac{\partial^2\phi_l}{\partial x^2} + \frac{\partial^2\phi_l}{\partial z^2}\right) = A\sin\phi_l + B(z)\sin 2\phi_l. \tag{3}$$

with

$$A = 2U - P_0E; \qquad B(z) = \frac{\varepsilon_0\Delta\epsilon E^2\sin^2\theta_0}{2} - w_0[\delta(z - d/2) + \delta(z + d/2)]. \tag{4}$$

We seek traveling-wave solutions of this equation to describe the advance of ferroelectrically ordered fingers into the antiferroelectric layers when a sufficiently strong electric field is applied. When there is no dependence on z in the function $B(z)$, then exact solutions to this equation may be found[5]. They are of the form

$$\phi(x,t) = 2\arctan e^{r(x - vt)} \tag{5}$$

where $r = \sqrt{-2B/k + A^2 I/k\gamma^2}$. For these to be valid, r must be real, which is always the case when the dielectric anisotropy $\Delta\epsilon$ is negative. When $A < 0$ they represent a rotation of ϕ from π to 0 as the finger advances; for positive A the velocity v is negative, and the ferroelectric finger recedes. These solutions have been shown[5] to be stable whenever $|A| < -2B$. The velocity of the solitary waves for constant B is

$$v = (E - E_{c2})\frac{P_0}{\gamma}\sqrt{\frac{k}{-2B + (E - E_{c2})^2 P_0^2 I/\gamma^2}}. \qquad (6)$$

The introduction of the z-dependence of B complicates the problem. Now the magnitude of B is larger at the surfaces than in the bulk. This causes the solitary wave to have the tendency to move faster in the bulk than at the surface. However, the curvature term $\partial^2\phi_l/\partial z^2$ tends to prevent the separation of the bulk behavior from the surface behavior. We have found that there is a critical value of the surface anchoring strength w_o at which the surface wave can become detached from the bulk wave.

This phenomenon is clearly seen in the results of the numerical solution of Eq. (3) for typical values of the parameters involved[2]. Figure 2 shows the initial arrangement, in which a solitary wave is present but for which there is no dependence on z. The rear of the figure marks the surface of the cell, and the vertical axis represents ϕ. The equation of motion is then integrated to yield the form of the wave at later times. The result when the anchoring is weak is shown in Fig. 3, and depicts a single traveling wave which exhibits only a small amount of variation with z as the wave moves to the right. When the strength of the anchoring is increased, on the other hand, one finds the result shown in Fig. 4. Now the behavior at the surface is quite different from that in the bulk, and one sees that there are two distinct waves propagating at different speeds. The surface wave proceeds at a slower speed than the bulk wave.

The results of the numerical solutions are summarized in Fig. 5, which shows the speed of propagation of the solitary waves as a function of anchoring strength. When w_o exceeds a certain critical value, there are two possible velocities with which the waves can advance. For a typical experimental situation this critical anchoring strength is likely to be of the order of $10^{-5}\mathrm{J/m^2}$. The speed of the bulk wave is quite insensitive to the anchoring strength, and changes by little more than a per cent as the value of w_0 is increased. The surface wave, on the other hand, travels with a velocity that soon becomes very small, effectively vanishing by the time the anchoring has increased by 50% above its critical value. In addition, the effects of surface imperfections have not been taken into account in this calculation. Because one can expect to find some degree of pinning at the surface, the velocity of the surface-anchoring wave may drop even more precipitously to zero at some intermediate point in a real system.

We thank J. F. Li and C. Rosenblatt for helpful discussions. This work was supported by the ALCOM NSF Science and Technology Center under Grant DMR 89-20147.

REFERENCES

1. J. F. Li, X. Y. Wang, E. Kangas, P. L. Taylor, C. Rosenblatt, Y. Suzuki and P. E. Cladis, Phys. Rev. B **52**, R13075 (1995).
2. X. Y. Wang and P. L. Taylor, Phys. Rev. Lett. **76**, 640 (1996).
3. See, for a recent review, A. Fukuda, Y. Takanishi, T. Isozaki, and H. Takezoe, J. Mater. Chem. **4**, 997 (1994).
4. K. Miyachi, J. Matsushima, Y. Takanish, K. Ishikawa, H. Takezoe, and A. Fukuda, Phys. Rev. E **52**, R2153 (1995).
5. E. Magyari, Phys. Rev. B **29**, 7082 (1984).

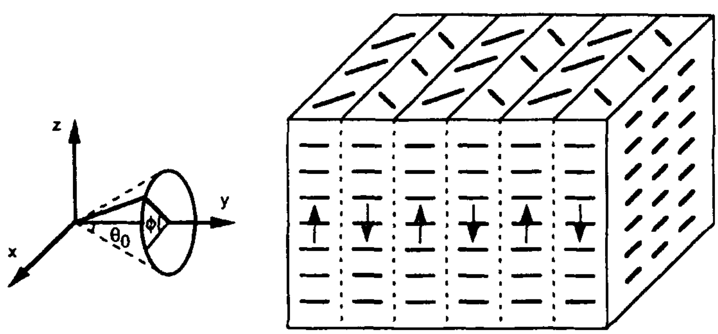

FIGURE 1. Geometry of the model antiferroelectric liquid crystal.

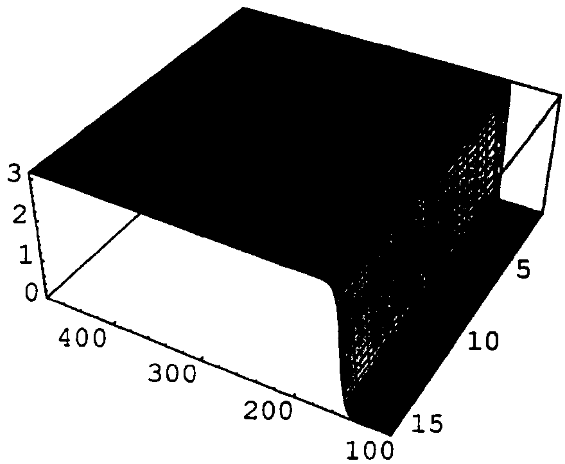

FIGURE 2. The starting configuration for ϕ, plotted vertically, is shown as a function of position along the propagation direction, plotted from right to left, and the distance from the cell surface, which is at the rear of the figure.

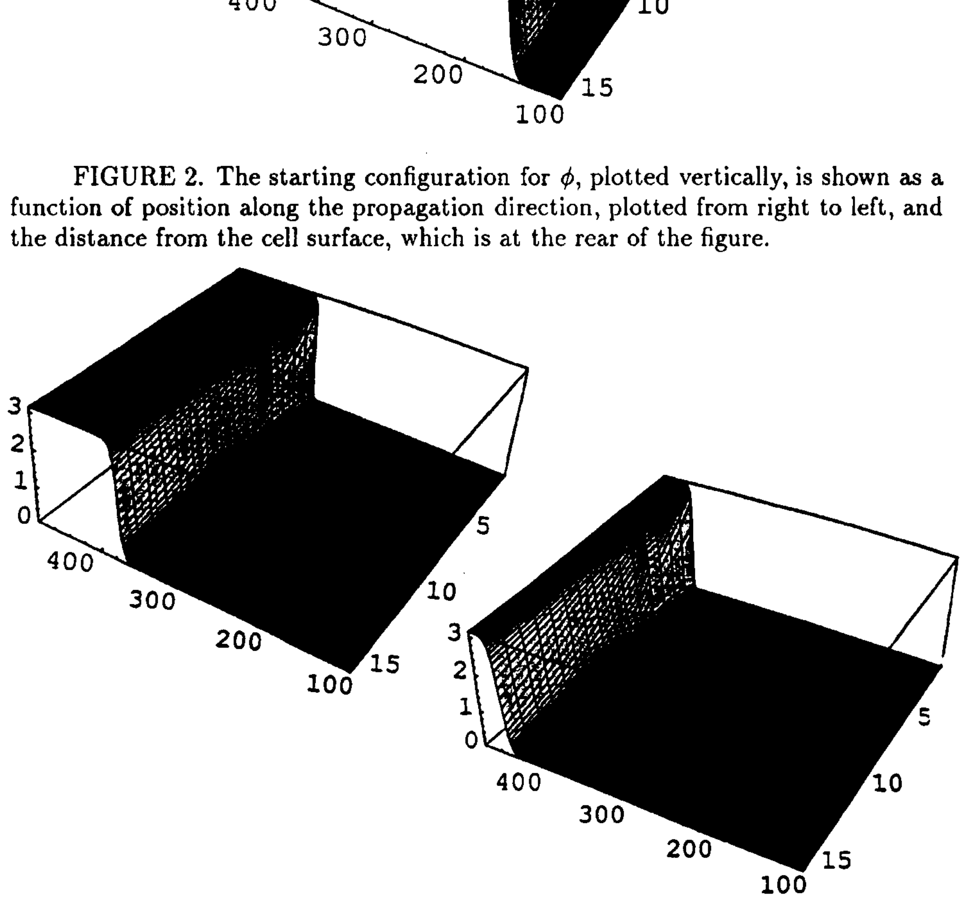

FIGURE 3. When the anchoring strength w_0 is $1.5\times10^{-5}\,J/m^2$, the wave whose initial form was as in Fig. 2 travels to the left with little variation in the z-direction. These surfaces show the wave after 6,000 and 8,000 iterations, respectively.

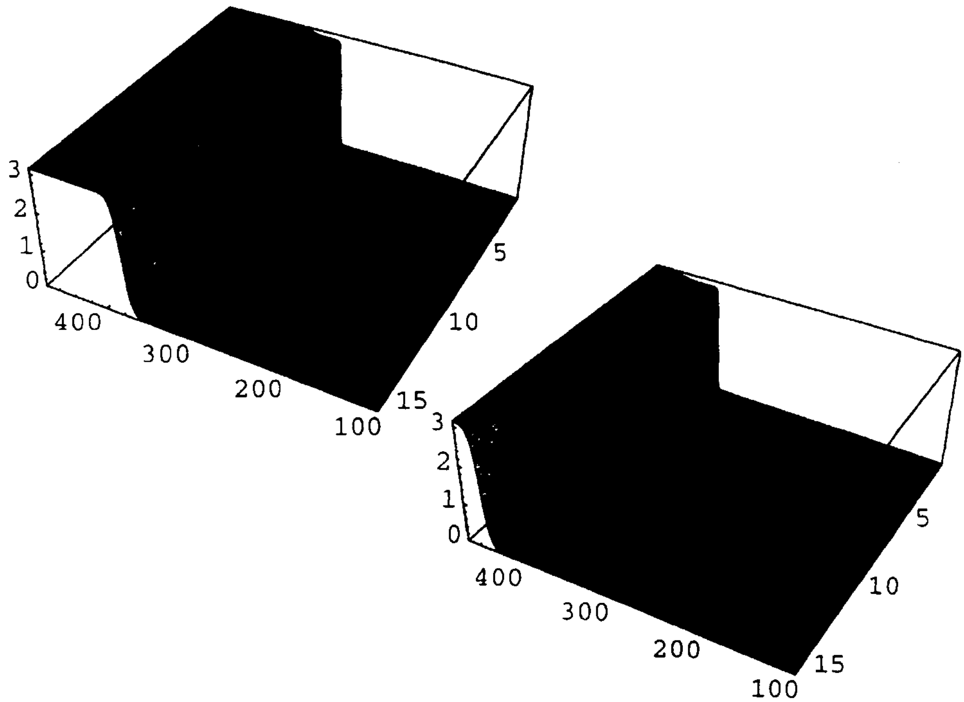

FIGURE 4. Increasing the anchoring strength w_0 to $2.5 \times 10^{-5} J/m^2$ causes the wave whose initial form was as in Fig. 2 to develop a significant variation in the z-direction as it travels. A slower-moving surface wave confined to the vicinity of the substrate has now detached itself from the faster-moving bulk wave. Again, these surfaces show the wave after 6,000 and 8,000 iterations, respectively.

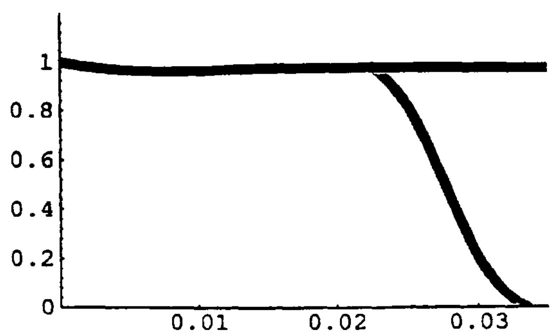

FIGURE 5. This schematic phase diagram shows the range of anchoring strength at which the surface waves can exist as entities distinct from the bulk waves. The ordinate shows the velocity of the wave in units of the zero-anchoring value, while the abscissa measures the anchoring for a typical system in units of mJ/m^2.